Features of excess conductivity and a possible pseudogap in FeSe superconductors

Cite as: Low Temp. Phys. **46**, 538 (2020); https://doi.org/10.1063/10.0001059
Submitted: 23 March 2020 . Published Online: 28 May 2020

A. L. Solovjov, E. V. Petrenko, L. V. Omelchenko, E. Nazarova, K. Buchkov, and K. Rogacki

Low Temperature Physics ARTICLE scitation.org/journal/ltp

Features of excess conductivity and a possible pseudogap in FeSe superconductors

Cite as: Fiz. Nizk. Temp. **46**, 638–652 (May 2020); doi: 10.1063/10.0001059
Submitted: 23 March 2020

A. L. Solovjov,[1,a)] E. V. Petrenko,[1] L. V. Omelchenko,[1] E. Nazarova,[2] K. Buchkov,[2] and K. Rogacki[3]

AFFILIATIONS

[1]B. Verkin Institute for Low Temperature Physics and Engineering, National Academy of Sciences of Ukraine, 47 Nauky Ave., Kharkov 61103, Ukraine
[2]Georgi Nadjakov Institute of Solid State Physics, Bulgarian Academy of Sciences, 72 Tsarigradsko Shosse Blvd., Sofia 1784, Bulgaria
[3]W. Trzebiatowski Institute of Low Temperatures and Structure Research, PAS Wroclaw, 1410 PL-50-050, Poland

[a)]**Author to whom correspondence should be addressed:** solovjov@ilt.kharkov.ua

ABSTRACT

The temperature dependence of excess conductivity $\sigma'(T)$ has been studied in three polycrystalline samples of the $FeSe_{0.94}$ superconductor, prepared by different technologies. The measured temperature dependences of the $\Delta^*(T)$ parameter, which is associated with the pseudogap in cuprates, were analyzed using the local pair model. At high temperatures, all three samples exhibit a high narrow maximum along $\Delta^*(T)$ at T_{s1}~250 K, which is typical for magnetic superconductors. Below $T \approx 225$ K, the dependences $\Delta^*(T)$ become different. Over almost the entire temperature range below T_{s1}, the S2 sample, prepared by solid state reaction without impurities, exhibits a $\Delta^*(T)$ that is typical for Fe-pnictides. An exception is the interval between the structural change temperature $T_s = 85$ K and T_c, where this $\Delta^*(T)$ exhibits an atypical, broad maximum. An analysis of the obtained dependence suggests the discovery of a pseudogap in this $FeSe_{0.94}$ sample, below T_s. Samples S1, containing 4 wt.%Ag, and S3, having a nominal composition but containing nonsuperconducting hexagonal phase inclusions, both prepared by partial melting, show identical $\Delta^*(T)$, but different from S2. They have a number of features that correlate with temperatures at which there are also features along $M(T)$, and the Hall coefficient $R_H(T)$ changes signs several times with decreasing T, which indicates that there is change in the type of charge carriers in FeSe. The $\Delta^*(T)$ dependence of the S3 sample below T_s has almost no maximum, since the nonsuperconducting impurities of the hexagonal phase in S3 prevent the formation of paired fermions near T_c. As a result, S3 also has the minimum local pair density $<n\uparrow n\downarrow> = 0.26$, determined by comparing $\Delta^*(T_G)/\Delta_{max}$ near T_c using the Peters–Bauer theory, whereas the dependence $\Delta^*(T)$ does not follow the theory. S1 has the maximum $<n \uparrow n \downarrow> = 0.47$, supposedly due to the influence of Ag impurities. In S2, which is pure, $<n \uparrow n \downarrow> \approx 0.3$, which is the same as that of $YBa_2Cu_3O_{7-\delta}$, and both dependences $\Delta^*(T)$ for S1 and S2 follow the theory over a wide temperature range.

1. INTRODUCTION

Despite the extremely large number of studies devoted to researching high-temperature superconductors (HTSCs), more than thirty years after their discovery there is still no clarity surrounding the superconducting (SC) pairing mechanism, which enables the formation of Cooper pairs at the SC transition temperature $T_c >> 100$ K.[1–3] Recently, there has been a noticeable surge of interest in studying the unusual phenomenon known as the pseudogap (PG),[4–10] which opens in cuprate HTSCs (cuprates) such as $YBa_2Cu_3O_{7-\delta}$ (YBCO) at a characteristic temperature $T^* >> T_c$.[3,11] It is believed that understanding the physics of the PGs would shed light on the SC pairing mechanism in HTSCs. However, the question of PG physics remains highly controversial.[5–14]

After superconductivity was discovered in FeSe chalcogenide,[15] which has the simplest structure among all HTSCs,[16–18] it was expected that answers to the abovementioned questions would be imminent. However, it is obvious that FeSe has a whole number of properties that are so unusual (see Refs. 13 and 18, and references therein), that the issues researchers were trying to tackle were not only not clarified, but, perhaps, became even more complicated. Indeed, the very dependence of the longitudinal resistivity $\rho(T)$ in FeSe is extraordinary, having a pronounced semiconducting behavior over a wide temperature range above ~315 K.[19,20] However, below ~300 K, $\rho(T)$ it exhibits a metallic course,[19,20] and assumes a form that is characteristic of weakly doped cuprates,[21,22] and iron-containing superconductors (Fe-pnictides)[13,23] As the temperature

decreases, FeSe becomes a superconductor with a SC transition temperature $T_c \approx 10$ K at normal pressure,[18–20,24] and in a very narrow range of Se concentrations.[25] It has been found that T_c can increase to 38 K when pressure of up to 9 GPa is applied.[26,27] A partial replacement of Se atoms with S or Te also contributes to an increase in T_c.[24,28,29] In some cases, the combination of pressure and intercalation can implement superconductivity at 48 K.[30] It is also reported that FeSe films one unit cell thick have a critical temperature that can reach about 109 K,[31–33] indicating that new unusual superconductivity can be observed in these compounds.[34]

Ultimately, it has been shown that the maximum along $\rho(T)$ that was observed in FeSe above 300 K[19,20] is neither related to the electron-phonon scattering, nor the interaction between spin fluctuations and charge carriers,[19] or their thermal activation.[35] Most likely, in the range of 350–300 K the electron band structure of FeSe is rearranged, which can lead to an increase in the charge carrier density n_f, and the observed decrease in $\rho(T)$ with dropping T, as a result (see Refs. 18 and 19 and references therein). It should also be noted that there are no reports of any structural or magnetic transition at 300 K.[19,20] A weakly pronounced structural transition is detected at $T_{s1} \approx 250$ K,[36,37] and a well-known structural transition is observed at $T_s \sim 90$ K.[24,25,38] However, unlike Fe-pnictides, this transition is not accompanied by a corresponding antiferromagnetic transition (see Refs. 18, 39, and 40, and references therein). For this reason, in many articles this behavior in FeSe is attributed to charge-induced nematicity.[16,19,24,41–43] Such a transition is associated with spontaneous symmetry breaking in the x and y directions in the Fe planes, which reduces the lattice symmetry group from tetragonal to orthorhombic. This fact reflects the internal electron instability of FeSe, and the complex evolution of the electron band structure with decreasing temperature, when the charge carriers change from electrons to holes, and vice versa.[18,19,36–43] This follows from measurements of the Hall and Seebeck coefficients, which change signs several times as the temperature decreases from 300 K, confirming the conclusion that FeSe is a compound with two types of charge carriers.[24,44,45] It can be assumed that FeSe compounds are in the crossover mode between BCS and Bose–Einstein condensation (BEC).[40,43,46,47]

The behavior of FeSe considered above differs significantly from that of cuprates, wherein $\rho(T)$ is a linear function in a broad temperature range above the pseudogap opening temperature $T^* >> T_c$.[11,12,22,48–50] Below T^*, the dependence $\rho(T)$ deviates from the linear toward lower values, which leads to the appearance of excess conductivity $\sigma'(T)$, defined as the difference between the measured conductivity $\sigma(T) = 1/\rho(T)$ and the extrapolated linear conductivity $\sigma_N(T) = 1/\rho(T)$, which corresponds to the normal state of the sample.[11,48,51,52] For YBCO, in a relatively narrow temperature range of ~15 K above T_c, the excess conductivity is well described by the Aslamazov–Larkin (AL)[53] and Hikami–Larkin (HL)[54] (Maki–Thompson contribution (MT)[11,48,52]) classical fluctuation theories. This is the region of SC fluctuations, bounded from above by the temperature T_{01},[11,52] and accordingly, the region of fluctuation conductivity (FLC), which is characterized by a nonzero superfluid density n_s[55–58] caused by the formation of fluctuation Cooper pairs (FCP) above T_c. In this temperature range, FCPs behave much like SC Cooper pairs, but without long-range order,[47,58] they are the so-called "short-range phase correlations," which should largely obey BCS theory.[47,55–59] The study of SC fluctuations as part of cuprate HTSC research has received a lot of attention (see Refs. 11, 48, 52, and 60, and references therein), since it was assumed that this is the best way to discover the nature of the pseudogap.[11,12,48–50,52]

Unlike cuprates, there are almost no studies of SC fluctuations in FeSe, due to the fact that it is extremely difficult to identify its normal state. As a result, there are practically no data on the existence of such FCPs above T_c in these compounds, or their possible effect on the abovementioned unusual properties of FeSe. As expected, the data on the possible implementation of the PG state in FeSe compounds, which are reported in a number of articles, are also highly contradictory.[44,61–66] In our previous article,[67] three polycrystalline samples of $FeSe_{0.94}$ prepared by various methods (S1, S2, and S3) are used to study the fluctuation conductivity $\sigma'(T)$ near T_c, as a function of temperature. It is shown that, as is the case in cuprates, the 3D-AL and 2D-MT (D is the dimension) fluctuation theories provide an excellent description of the $\sigma'(T)$ dependence in the SC fluctuation region that is observed up to ~20 K, which is approximately two times higher than T_c. This result, which unambiguously points to the presence of FCPs in FeSe, at least in the indicated temperature range, is in agreement with the earlier studies on magnetic susceptibility[46] and microcontact spectroscopy in FeSe single crystals.[68] Note that up to T_s~90 K there are no features (anomalies) along the $\rho(T)$ curves, which suggests that the fluctuation Cooper pairs can exist in FeSe, at least up to T_s.[44,61–63] Moreover, it is argued in a number of articles that the features of the PG should start to manifest directly below the structural transition temperature T_s, where the fluctuation effects suppress the density of states (DOS) at the Fermi level[69,70] by forming paired electrons above T_c,[63,71] which, by definition, is called a pseudogap.[3,5,11] This idea is supported by magnetoresistance experiments in FeSe, where the corresponding dependences at different values of the applied constant magnetic field do not obey Kohler's rule below T_s, pointing to the possible rearrangement of the Fermi surface.[45,46,63] However, the questions are: what happens to the FCPs above 20 K, and does a pseudogap state manifest in FeSe?

To provide clarification on these topics, a thorough examination of the excess conductivity in three samples of $FeSe_{0.94}$, prepared via different methods (S1, S2, and S3) is performed in this article, to glean information about the magnitude and temperature dependence of the possible PG, $\Delta^*(T)$. The calculated dependences $\Delta^*(T)$ have turned out to be typical for magnetic superconductors.[23,72] It is shown that the features manifesting along $\Delta^*(T)$ are in good agreement with the results obtained by other research methods (see Refs. 18, 24, 44, and 45, and references therein). A comparison with the Peters–Bauer theory[73] is used to estimate the local pair density in the studied samples near T_c, and determine the relationship between the local pairs and the structural features of the studied polycrystalline samples. A detailed review of the obtained results is given below.

2. THE EXPERIMENT

Three $FeSe_{0.94}$ samples are prepared using various techniques. The synthesis of the $FeSe_{0.94}$ samples used in this study is detailed in Ref. 74. Samples S1, containing 4 wt.%Ag, and S3 without silver

additives, were obtained using the partial-melting technique. Sample S2, with a nominal composition of $FeSe_{0.94}$, was obtained via solid state reaction (SSR).

Silver is widely used as a dopant, or small additive, in order to improve microstructure and superconducting properties.[75–77] Our previous studies established that a small amount of silver added to $FeSe_{0.94}$ granules augmented both the internal and intergranular SC properties.[74,78] This consists of increasing the T_c, the upper critical field $H_{c2}(0)$, the Ginzburg–Landau parameter κ, the critical current and pinning energy, as well as decreasing the width of the SC resistive transition ΔT_c.[79]

Powder X-ray diffraction (XRD) patterns are collected within the range of 5.3 to 80° 2θ with a constant step 0.02° 2θ on a Bruker D8 Advance diffractometer with CuK_α radiation and a LynxEye detector. The composition is studied using Diffracplus EVA and the ICDD-PDF2 database.[74] It is found that both undoped samples S2 and S3 consist mainly of the SC tetragonal phase. However, the S3 sample prepared by partial melting, shows inclusions of a nonsuperconducting hexagonal phase. At the same time, the S1 sample, which was also prepared using partial melting but doped with Ag, shows no trace of the hexagonal phase. Only a small amount of Ag was identified as an impurity. Thus, similarly to Sn additives in FeSe,[80] Ag prevents the formation of a nonsuperconducting hexagonal phase and increases the content of the SC tetragonal phase in the sample. At the same time, the lattice parameters determined from XRD measurements for the S1 and S3 samples are the same: S3: $a = 3.7650$ Å, $c = 5.5180$ Å, and S1: $a = 3.7671$ Å, $c = 5.5193$ Å. This confirms the earlier conclusion that Ag most likely does not integrate into the unit cell.[77] The parameters of sample S2 are also almost the same: $a = 3.77598$ Å, $c = 5.51800$ Å. The FeSe unit cell is a tetrahedron in which the Fe ion is in the center, and Se ions are at its vertices, which corresponds to the space group *P4/nmm* with parameters $a = 3.77$ Å (Fe–Fe distance) and $c = 5.52$ Å (interplanar distance), with the height of Se ions over the Fe planes $z_{Se} = 0.2343$ (~ 1.45 Å).[19,25,28] Thus, the parameters of the $FeSe_{0.94}$ samples measured by us correspond to literature data.

Rectangular samples with dimensions of about $5 \times 1 \times 1$ mm are cut from pressed tablets. The longitudinal resistivity ρ_{xx} is measured using a standard four-probe circuit on the automated Quantum Design PPMS-14 T system. Silver paste is used to secure thin wires to the edges of the sample, to ensure a uniform distribution of current in the central region where the potential probes with a width of less than 0.3 mm are placed. The contact resistance of the potential probes is less than 1 Ω. It is expected that the samples in our experiments will have different behaviors as a result of the varying preparation methods, and the features of the pseudogap parameter temperature dependence $\Delta^*(T)$ obtained by measuring the resistivity and excess conductivity, will be analyzed.

3. RESULTS AND DISCUSSION

3.1. Resistive properties

Figure 1 shows the temperature dependences of the resistivity $\rho(T) = \rho_{xx}(T)$ for all three studied $FeSe_{0.94}$ samples. It is seen that all $\rho(T)$ dependences exhibit metallic behavior as the temperature decreases to T_c. The critical temperature $T_c \equiv T_c$ ($\rho = 0$) is determined by extrapolating the linear part of $\rho(T)$ in the region of the

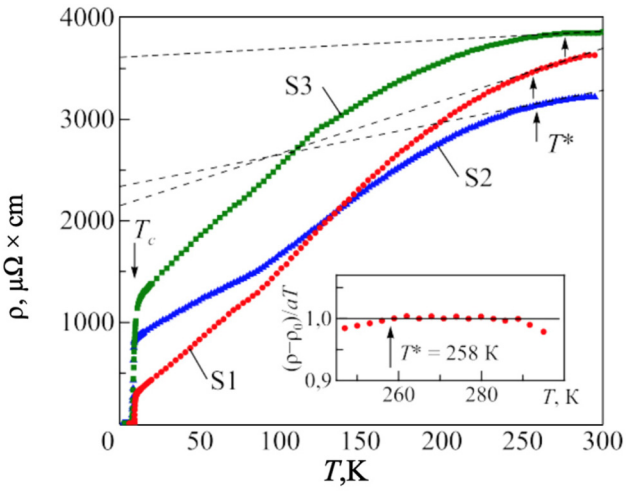

FIG. 1. The temperature dependences of resistivity $\rho(T)$ for all three $FeSe_{0.94}$ samples (S1, S2, and S3) prepared via different methods (see text). The dotted lines represent the $\rho_N(T)$ extrapolated to the low temperature region. Insert: $(\rho - \rho_0)/aT$ as a function of temperature for S1 (dots), defining $T^* = 258$ K. A straight line is drawn for clarity.

SC transition to $\rho(T) = 0$. Since the width of the resistive transitions, ΔT_c, turns out to be quite small, especially in the case of S1 ($\Delta T_c \sim 1$ K),[74] this approach allows us to obtain T_c values with a high degree of accuracy. As expected, the sample doped with silver (S1) has the highest $T_c = (9.0 \pm 0.05)$ K and the lowest ρ ($T = 10$ K) ≈ 270 μΩ × cm (Table I). In addition, S1 has the largest resistance ratio $R(300\text{ K})/R(10\text{ K})$, or RRR = 13.6.[45] This RRR value is significantly higher than that observed in the case of polycrystalline FeSe samples obtained by the self-flux method, where RRR = 9.3,[44] which confirms the high quality of the S1 sample structure.

Accordingly, sample S3 has a noticeably lower $T_c = (7.8 \pm 0.05)$ K and the highest $\rho(T = 10\text{ K}) \approx 1010$ μΩ × cm (Table I). Most likely, this is caused by inclusions of the nonsuperconducting hexagonal phase detected by XRD analysis,[74] which can distort the sample's structure.

Accordingly, the S3 RRR = 3.8. Interestingly enough, despite all of the mentioned differences, the samples S1 and S3 obtained by partial melting have similarly shaped $\rho(T)$ dependences (Fig. 1). Additionally, below ~ 150 K, both resistive curves run parallel to each other. The lowest $T_c = (7.7 \pm 0.05)$ K is observed for sample S2 that was obtained by the solid state reaction method. Therefore, in this case, $\rho(T = 10\text{ K}) \approx 838$ μΩ × cm, which is noticeably larger than that of S1, and RRR = 3.9 (Table I), which points to the structural features of the sample that are caused by its preparation method. As a result, S2 has a differently shaped $\rho(T)$ curve, which passes below $T_s = 85$ K, with a slope that is noticeably smaller than that of samples S1 and S3. This confirms the assumption that the properties of FeSe polycrystalline samples substantially depend on the method of their preparation.[63] We expected there to be differences in the samples' structural features, and in the study of a possible pseudogap in FeSe.

TABLE I. Parameters of S1-S3 $FeSe_{0.94}$ samples, obtained by analyzing the fluctuation conductivity and $\Delta^*(T)$.

Sample	ρ(10 K), μΩ×cm	RRR	T_c, K	$\xi_c(0)$, Å	T^*, K	ε^*_{c0}	A_4	$\Delta^*(T_G)$, K	T_{pair}, K	$2\Delta^*(T_G)/k_BT_c$
S1	270	13.6	9.0	2.9	258	6.3	13.0	13.3	70	3.0
S2	838	3.9	7.7	2.9	259	10.0	7.4	17.7	53	4.6
S3	1010	3.8	7.8	5.6	273	10.0	7.9	10.2	–	3.0

3.2. Excess conductivity and the pseudogap

The magnitude and temperature dependence of the pseudogap parameter $\Delta^*(T)$ for all three samples is calculated in the local pair (LP) model[11] based on excess conductivity $\sigma'(T)$ measurements. As noted above, $\sigma'(T)$ is determined by the equation

$$\sigma'(T) = \sigma(T) - \sigma_N(T) = \frac{1}{\rho(T)} - \frac{1}{\rho_N(T)}. \quad (1)$$

This shows that finding the normal state of the HTSC, which determines the magnitude and temperature dependence of the resistivity $\rho_N(T)$, is extremely important for determining $\sigma'(T)$ and therefore, $\Delta^*(T)$.[11] In cuprates, $\rho_N(T)$ is a linear function of T over a wide temperature range above T^*.[21,22] According to the NAFL (Nearly Antiferromagnetic Fermi-liquid) model,[51] this linear dependence corresponds to the normal state of HTSC, which is characterized by Fermi surface stability. Below T^* $\rho(T)$ deviates from the linear dependence toward smaller values, leading to the appearance of excess conductivity, and the HTSC transitions to the PG state (see Refs. 11, 18, and 48, and references therein). According to the latest concepts,[4,14,49] the rearrangement of the Fermi surface, which largely determines the unusual properties of cuprates in the PG region, is possible below T^*.

In contrast to cuprates, the normal state of FeSe is rather undefined. Ultimately, the chosen normal state is shown by the dashed lines in Fig. 1, based on the considerations detailed in our previous work.[67] Let us note only a few points. As already mentioned, the rearrangement of the band structure ends below ~ 300 K, and FeSe transitions to a new state that is characterized by metallic charge carrier scattering.[18–20,39] It has been found that in this state, the Hall coefficient R_H is practically independent of temperature,[19,26,45] and the field-dependent magnetoresistance $MR = [\rho(H) - \rho(0)]/\rho(0)$, measured at various temperatures, obeys Kohler's rule up to $T_s \approx 85$ K.[45,81] Both results indicate the stability of the Fermi surface in FeSe for this temperature range, which, as noted above, is the main sign of the normal state of any HTSC. Moreover, in the relatively short temperature range of ~ 30 K below 290 K, the $\rho(T)$ dependence of all samples turns out to be linear. Here, we used the criterion $[\rho(T) - \rho_0]/aT = 1$, obtained by transforming the straight line equation $\rho(T) = aT + \rho_0$, where a is the slope of the extrapolated dependence $\rho_N(T)$, and ρ_0 is its intersection with the Y axis.[1,21,52] In this case, the deviation of $[\rho(T) - \rho_0]/aT$ from 1, as shown by the insert in Fig. 1 for S1 as an example, allows one to determine T^* with a high degree of accuracy. We note that this approach to determining $\rho_N(T)$ made it possible to obtain reasonable and self-consistent results, and to confidently observe both AL and MT fluctuation contributions to $\sigma'(T)$ when analyzing the fluctuation conductivity.[67] However, the question of possibly realizing the pseudogap state in FeSe turned out to be much more complicated.[44,46,61–66]

3.3. Analyzing the dependence Δ*(T)

It is believed that in cuprates, the excess conductivity $\sigma'(T)$ [Eq. (1)] arises as a result of the PG opening and, therefore, must contain information about its magnitude and temperature dependence. We also share the opinion that the PG in cuprates arises due to the formation of local pairs at $T < T^*$.[6–11,47,58,62,82] Classical fluctuation theories such as AL[53] and MT, which were modified by Hikami and Larkin (HL)[54] for HTSCs, provide a perfect description of the experimental $\sigma'(T)$ in cuprates, but only in the range of SC fluctuations $\Delta T_{fl} = T_{01} - T_c^{mf} \approx 15$ K[52] (the definition of T_c^{mf} is given below). It is obvious that in order to get information about the PG, we need an equation that describes the entire experimental curve from T^* to $\sim T_c^{mf}$, and contains the PG $\Delta^*(T)$ parameter in explicit form. In the absence of a rigorous fundamental theory, such an equation was proposed in Ref. 82:

$$\sigma'(T) = \frac{e^2 A_4 (1 - T/T^*)(\exp(-\Delta^*/T))}{16\hbar\xi_c(0)\sqrt{2\varepsilon^*_{c0}\mathrm{sh}(2\varepsilon/\varepsilon^*_{c0})}}, \quad (2)$$

where $(1-T/T^*)$ and $\exp(-\Delta^*/T)$ take into account the dynamics of LP formation at $T \le T^*$ and their destruction near T_c, respectively. A_4 is a numerical coefficient that has the meaning of the C-factor in the FLC theory, and $\Delta^* = \Delta^*(T_G)$ is the value of the PG parameter near T_c.[11,82–84]

Solving Eq. (2) with respect to $\Delta^*(T)$, we obtain

$$\Delta^*(T) = T \ln \frac{e^2 A_4 (1 - T/T^*)}{\sigma'(T) 16\hbar\xi_c(0)\sqrt{2\varepsilon^*_{c0}\mathrm{sh}(2\varepsilon/\varepsilon^*_{c0})}}, \quad (3)$$

where $\sigma'(T)$ is the experimentally measured excess conductivity over the entire temperature range from T^* to T_c^{mf}.

Let us note once again that in HTSC cuprates, not only do all of the sample parameters change at $T \le T^*$, but the DOS at the Fermi level also begins to decrease,[69,70] i.e., a pseudogap opens.[3–11] It is assumed that this also involves the rearrangement of the Fermi surface[4,14,49,51], which breaks up into Fermi arcs below T^*.[4,70] It is assumed that a correct understanding of the PG physics would also reveal the SC pairing mechanism in HTSCs, which remains obscure.[4,11,47,49,58,62,73] However, we do not know of any DOS measurements that have been performed for FeSe. Therefore, the

question of PG manifestation in such HTSCs remains open. In the absence of other theories, we analyze $\sigma'(T)$ and $\Delta^*(T)$ in FeSe using local pairs, Eqs. (2) and (3). The temperature at which $\rho_N(T)$ deviates from linearity, 258 K, is denoted as T^*, although there is no strong evidence to suggest that this is the temperature at which the PG opens in FeSe. For the same reason, we are not referring to the parameter $\Delta^*(T)$, which we find by analyzing excess conductivity over the interval from T^* to T_c, as a pseudogap.

Equations (2) and (3) contain a number of parameters which, importantly, can be experimentally determined.[11,52,82] As such, T^*, the coherence length along the c axis $\xi_c(0)$, and the reduced temperature $\varepsilon = (T - T_c^{mf})/T_c^{mf}$ are all determined by analyzing the resistivity and the FLC.[52,67,72] Here, T_c^{mf} is the critical temperature in the mean-field approximation, which separates the FLC region from the critical fluctuation region, or fluctuations of the SC order parameter Δ right near T_c, not accounted for in the Ginzburg–Landau theory.[85,86] To find T_c^{mf}, we use the fact[11,21,23,52] that in all HTSCs, near T_c, $\sigma'(T)$ is always described by the standard equation of the 3D-AL theory,[53] in which $\sigma'_{AL3D} \sim \varepsilon^{-1/2} \sim (T - T_c^{mf})^{-1/2}$. Accordingly, T_c^{mf} is determined by linearly extrapolating the dependence σ'^{-2} on T in the 3D fluctuation to its intersection with the temperature axis, since $\sigma'^{-2} = 0$ when $T \to T_c^{mf}$.[84] Let us note that it is always $T_c^{mf} > T_c$. The Ginzburg temperature is another characteristic, and it is the point until which the fluctuation theories are applicable $T_G > T_c^{mf}$. This temperature is usually determined by the Ginzburg criterion, which refers to the case when the mean-field theory stops describing the SC transition[87,88]. It is important that other parameters, such as the theoretical parameter ε_{c0}^*,[1] coefficient A_4, and $\Delta^*(T_G)$, can also be experimentally determined in the LP model.

Figure 2 shows the dependence of ln σ' on ln ε for sample S2, over the entire temperature range from T^* to T_c^{mf}, which shows that in the temperature interval from $T_{c01} = 24.9$ K to $T_{c02} = 94.9$ K, indicated in the figure by arrows at ln $\varepsilon_{c01} = 0.69$ and ln $\varepsilon_{c02} = 2.34$, $\sigma'^{-1} \sim \exp \varepsilon$.[89] This feature turns out to be one of the main properties of most HTSCs.[11,52,82,90] As a result, in the interval $\varepsilon_{c01} < \varepsilon < \varepsilon_{c02}$ (insert in Fig. 2), ln σ'^{-1} is a linear function of ε with a slope of $\alpha^* = 0.10$, which determines the parameter $\varepsilon_{c0}^* = 1/\alpha^* \approx 10$[89](Table I). This approach makes it possible to obtain reliable values of ε_{c0}^* for all other samples, which are also given in Table I. As established in Refs. 11, 52, and 82, this parameter significantly affects the shape of the theoretical curves shown in Figs. 2 and 3 at $T >> T_{01}$, i.e., significantly higher than the SC fluctuation region.

To determine the coefficient A_4, it is also necessary to know the value $\Delta^*(T_G)$ used in Eq. (2), which is found by combining the theory with experimental points, constructed as ln σ' as a function of $1/T$ (see Fig. 3). As can be seen in Refs. 21, 52, and 82, for example, in these coordinates the shape of the theoretical curve turned out to be very sensitive to $\Delta^*(T_G)$. In addition, it is assumed that $\Delta^*(T_G) = \Delta(0)$, where Δ is the SC gap.[57,91] Let us emphasize that it is precisely the $\Delta^*(T_G)$ value that determines the true value of the PG, and is used to estimate the value of the BCS ratio $2\Delta(0)/k_BT_c = 2\Delta^*(T_G)/k_BT_c$ in a specific HTSC sample.[21,52,82] The best approximation of ln σ' at a function of $1/T$ by Eq. (2) for sample S2 is achieved at $2\Delta^*(T_c)/k_BT_c = 4.6 \pm 0.2$, which slightly exceeds the limit of the BCS theory for d-wave superconductors ($2\Delta/k_BT_c \approx 4.28$).[92,93]

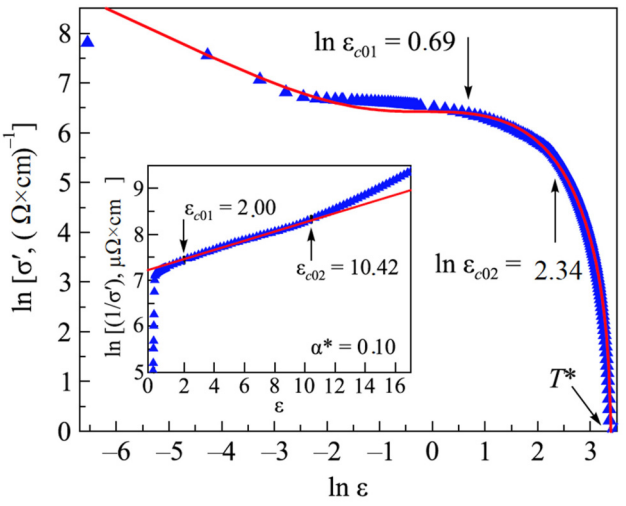

FIG. 2. The dependence of ln σ' on ln ε of sample S2 (triangles) over the entire temperature range from T^* to T_c^{mf}. The curve is the extrapolation of the experiment using Eq. (2). Insert: the dependence of ln σ'^{-1} on ε. The straight line denotes the region of the linear dependence from ε_{c01} to ε_{c02}. The slope α^* determines the parameter $\varepsilon_{c0}^* = 1/\alpha*$ (see text).

As we know (see Ref. 94, and references therein), cuprates have an abnormally large energy gap $\Delta(0) = \Delta_0$; therefore, the ratio $2\Delta/k_BT_c \sim 5$–7 is noticeably larger than that of the BCS theory for d-wave superconductors.[92,93] Among the theories that explain the large values of $2\Delta/k_BT_c$ in the tight binding limit,[95–97] the most

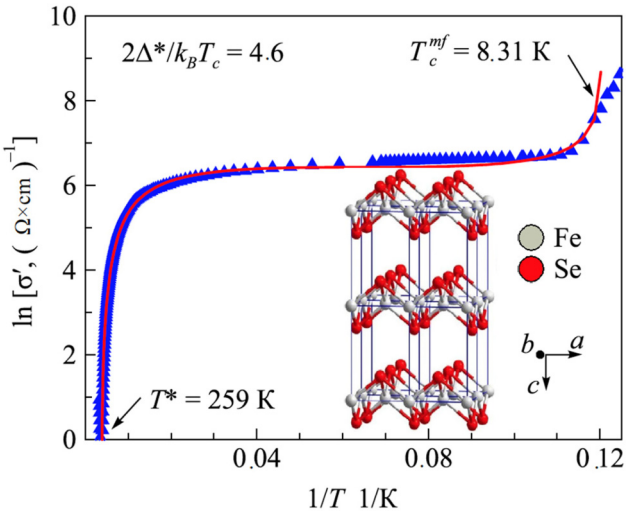

FIG. 3. ln σ' as a function of $1/T$ for sample S2 (triangles) in the temperature range from T^* to .T_c^{mf} The curve is an extrapolation of the experiment using Eq. (2). The insert shows the FeSe structure that corresponds to the conducting tetragonal phase.[106]

popular model is the one in which Cooper pairing in HTSCs is implemented by the interaction between electrons with spin fluctuations.[98–100] However, recent results obtained by angle-resolved photoemission spectroscopy (ARPES)[101] and scanning tunneling spectroscopy[102–104] have shown that HTSCs can have a weakly coupled pairing mechanism, because the critical temperature T_c is determined by the parameter Δ_{SC}, which is significantly less than Δ_0. As a result, the ratio $2\Delta_{SC}/k_BT_c \sim 4.3$, which corresponds to a *d*-wave BCS superconductor.[92,93] In this case, the low-frequency spin excitations at the basis of the spin-fluctuation model do not play a decisive role. In addition, there are also other models;[3–11,73] therefore, the question as to the value of $2\Delta/k_BT_c$ in HTSCs remains open.

The mechanism that implements the SC state in FeSe seems to be even more complex. A number of studies report the existence of two[105,106] and even three[107] energy gaps in FeSe, which is a consequence of these compounds' complex band structure. Corresponding calculations show that the Fermi surface (FS), in $FeSe_{0.85}$ for example,[106] is quasi-two-dimensional and consists of hole-like sheets around point Γ, and electron-like sheets around point *M* of the Brillouin zone.[108] Accordingly, it can be assumed that two different gaps open up on the different sheets of the FS. The ratios $2\Delta/k_BT_c$ obtained in the indicated papers are between 4.3 and 4.6 for the large gap, and between 1 and 2 for the small gap. Moreover, an analysis of the magnetic field penetration depth in the ab plane, λ_{ab}, using muon-spin rotation (μSR), showed that the value $2\Delta/k_BT_c$ depends substantially on the model chosen to interpret the obtained data results. It has been convincingly shown that the best agreement between the experimental data and theory is achieved by the two-gap $s+s$-wave model, for which the ratio $2\Delta/k_BT_c$ is 4.49 and 1.07 for the large (Δ_1) and small (Δ_2) gaps, respectively (see Ref. 106, and references therein). At the same time, it is emphasized that the superconducting gap in FeSe does not contain zeros, which is also noted in Ref. 105. Thus, the value $2\Delta^*/k_BT_c = 4.6 \pm 0.2$ obtained by us for S2 is in complete agreement with the results of Refs. 105–107 for the large gap, which confirm the correctness of our choice of approach to the analysis of excess conductivity in FeSe. The dependences of ln σ′ on 1/*T*, similar to those shown in Fig. 3, were obtained for samples S1 and S3. In both cases, the best approximation of ln σ′ as a function of 1/*T* by Eq. (2) is achieved at $2\Delta^*/k_BT_c = 3.0 \pm 0.2$. This is smaller than that of sample S2, but noticeably larger than that obtained in Refs. 105–107 for the small gap, where $2\Delta_2/k_BT_c = 1.07 \pm 0.3$.[106,107] This is how we experimentally measure the large gap in FeSe. In samples S1 and S3, it is substantially smaller than in S2, most likely due to a change in the FS due to the influence of Ag impurities (S1) or nonsuperconducting phase inclusions (S3).

Now that ε^*_{c0} and $\Delta^*(T_G)$ are known, we can return to our analysis and find the coefficient A_4, which is determined by calculating σ′(ε) using Eq. (2). By choosing A_4, we combine the theory with the experiment in the 3D AL fluctuation region near T_c, where ln σ′(ln ε) is the linear function of the reduced temperature ε with the slope $\lambda = -1/2$[11,82,83] (Fig. 2). As can be seen in the figure, Eq. (2) with $A_4 = 7.4$, $\varepsilon^*_{c0} = 10$, and $\Delta^*(T_G)/k_B = 2.3T_c = 17.7$ K, provides a good description of the experiment at temperatures between T^* and T_G, as expected. The only exception is the temperature range from T_0 to T_{c01} ($\ln \varepsilon_{c01} = 0.69$ in Fig. 2), where, in contrast to cuprates, it is assumed that magnetism has an enhanced influence on 2D fluctuations,[67] which are not accounted for by our model. The fact that σ′(*T*) is well described by Eq. (2) (Fig. 2), suggests that Eq. (3) will give a reliable value and temperature dependence of the Δ* parameter. Figure 4 displays the result of analyzing the Δ*(*T*) for sample S2 according to Eq. (3), using the following experimentally determined parameters: $T^* = 259$ K, $\xi_c(0) = 2.9$ Å, $\varepsilon^*_{c0} = 10$, $A_4 = 7.4$, and $\Delta^*(T_G)/k_B = 17.7$ K. Also shown are the dependences Δ*(*T*) for samples S1 and S3, constructed with an analogous set of parameters whose values are given in Table I. We assumed that the temperature dependences Δ*(*T*) can provide an answer to some of the questions outlined above.

The obtained dependences with a narrow maximum at $T_{max} = T_{s1} \approx 250$ K are typical for magnetic HTSCs like $EuFeAsO_{0.85}F_{0.15}$,[23] $Dy_{0.6}Y_{0.4}Rh_{3.85}Ru_{0.15}B_4$,[72] and $SmFeAsO_{0.15}$,[109] and differ substantially from analogous dependences Δ*(*T*) for nonmagnetic cuprates.[11,82,90] Below T_{s1} (Fig. 4), the Δ*(*T*) of all samples decreases rapidly, and a minimum is observed at $T_s \approx 85$ K. In FeSe compounds, this minimum corresponds to a structural phase transition from the tetragonal to the orthorhombic phase at T_s (see Refs. 18, 24, 45, and 63, and references therein). Below T_s, the parameter Δ*(*T*) increases slightly, demonstrating a maximum at T_{max}, followed by a minimum at T_G. The insert on Fig. 4 explains why this a minimum. It shows the dependences Δ*(*T*) for all samples in the SC fluctuation region near T_c. The Δ*(*T*) dependences for S1 and S2 are typical of the HTSCs we are considering, including cuprates and Fe-pnictides (see Ref. 52, and references therein). A minimum is always observed at $T \sim T_{01}$, which restricts the SC fluctuation region from above. Then, a maximum follows near the temperature T_0, at which there is a crossover from 2D MT fluctuations to 3D AL fluctuations.[52,67] Finally, there is a

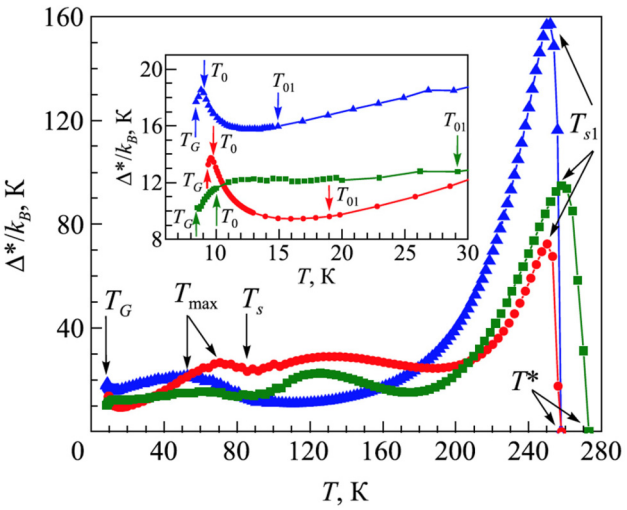

FIG. 4. The temperature dependences of the $\Delta^*(T)/k_B$ parameter of samples S1 (dots), S2 (triangles), and S3 (squares). Solid thin curves are shown for clarity. The insert shows the same dependences $\Delta^*(T)/k_B$ in the SC fluctuation region near T_c.

minimum at $T = T_G$. As we can see, sample S3 is the only exception. Its behavior does not match the general picture, likely due to the inclusions of the nonsuperconducting hexagonal phase.

The most clearly marked features at T_s and T_{max} are observed along the dependence $\Delta^*(T)$ for sample S2, which does not contain any dopants. Samples S1 and S3 demonstrate a number of additional features, which are particularly visible in Fig. 5, where $\Delta^*(T)$ is plotted in Δ^*/Δ^*_{max} units. Interestingly, these features correlate with the features on the temperature dependences of magnetization, $M(T)$, measured for S1 (dots) and S2 (triangles). As already noted, there is a pronounced maximum below T^* at $T_{s1} \approx 250$ K. A number of studies note the possibility of an additional, poorly studied structural transition in FeSe at this temperature.[36,37] It is seen that both $M(T)$ dependences have a feature at $T = T_{s1}$, which points to the possibility of rearranging the magnetic subsystem of $FeSe_{0.94}$ at $T_{s1} \sim 250$ K. Let us emphasize that this experimental fact is another reason to believe that the normal state in the studied $FeSe_{0.94}$ samples has been chosen correctly (see Sec. 3.2). In the temperature range from T_{s1} to ~ 225 K temperature range, the dependences $\Delta^*(T)$ of all three samples are decreasing linear functions of T (Fig. 5). It should be noted that a very similar linear dependence of $\Delta^*(T)$ is observed in a textured $EuFeAsO_{0.85}F_{0.15}$ polycrystalline sample with a close $T_c = 11.0$ K.[23] Importantly, in Fe-pnictides this linear dependence is observed clearly in the interval between the structural transition temperature T_s and the temperature of the spin-density wave transition (SDW), $T_{SDW} \sim 130$ K.[23,109] Thus, there is a similarity in the behavior of $\Delta^*(T)$ of FeSe and Fe-pnictides. In both cases, the linear dependence $\Delta^*(T)$ begins at the structural transition temperature. Whether FeSe has a transition to the SDW regime below ~ 225 K is not clear — since $M(T)$ has no features, this question remains open. Figure 5 shows that the dependences $\Delta^*(T)$ of samples

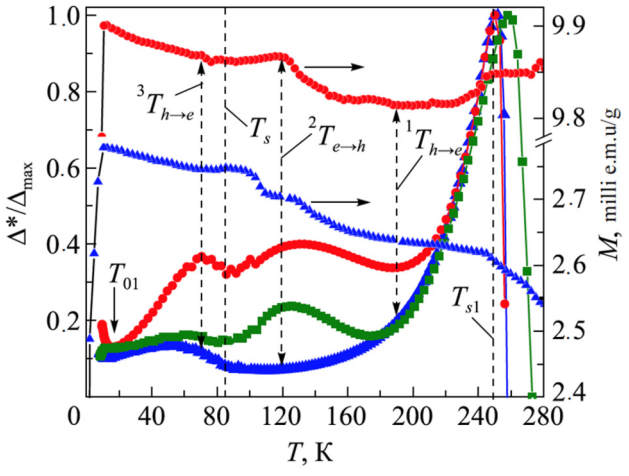

FIG. 5. The temperature dependences of Δ^*/Δ_{max} for S1 (dots), S2 (triangles), and S3 (squares), as well as the $M(T)$ curves of S1 (points) and S2 (triangles) (smaller characters). Solid thin curves are drawn for clarity. Vertical dashed lines without arrows indicate structural transitions at T_{s1} and T_s, and dashed lines with two arrows correspond to temperatures at which the charge carrier type changes (see text).

S1, S3 and S2 diverge below $T \approx 225$ K. Let us emphasize that, below this temperature, the shapes of the $\Delta^*(T)$ dependences for S1 and S3 obtained by partial melting are practically identical, with the exception of the SC fluctuation region (insert in Fig. 4). At the same time, they differ markedly from the $\Delta^*(T)$ of S2, obtained via solid state reaction, without any impurities.

Samples S1 and S3 have a minimum along $\Delta^*(T)$ near ~ 190 K that is absent for S2, the $\Delta^*(T)$ of which continues to decrease monotonously. One can assume that at $T \sim 225$ K, the charge carriers in FeSe start to change from hole to electron, which ends with a change in the Hall coefficient's sign, $R_H(T)$, at $^1T_{h\to e} \sim 190$ K, marked with a vertical dash in the figure (see Refs. 24 and 45, and references therein). At $^2T_{e\to h} \sim 120$ K, the $\Delta^*(T)$ of S1 and S3 has a pronounced maximum, which is also observed on $M(T)$ for S1. At the same time, the $\Delta^*(T)$ of S2 continues to decrease monotonously, approaching a minimum. However, S2 has a feature along $M(T)$. We note that at this temperature, the FeSe $R_H(T)$ changes signs again, meaning the charge carriers switch from electrons to holes Refs. 24 and 45. At $T_s \sim 85$ K, the rotational symmetry of FeSe decreases from fourfold (C4) to twofold (C2) as the crystal structure transitions from the tetragonal to the orthorhombic phase.[110] At the same time, it is assumed that an electronic order parameter is responsible for this transition.[111] Accordingly, at $T_s \sim 85$ K there is a minimum along the $\Delta^*(T)$ of all three samples, but there are no obvious features on the $M(T)$ curves (Fig. 5). The latter result is consistent with the idea that the FeSe structural transition at T_s is nematic.[16,18,24,41–46]

As the temperature decreases further, S1 demonstrates a specific asymmetric maximum along $\Delta^*(T)$ at a temperature of $^3T_{h\to e} = 70$ K, indicated by the dotted line in the figure, below which $\Delta^*(T)$ decreases rapidly in an almost linear way to T_{01} (see insert in Fig. 4). S3 shows a similar dependence of $\Delta^*(T)$ below T_s, but all the features are much less pronounced. At the same time, there are no features at $^3T_{h\to e} = 70$ K on $\Delta^*(T)$ for S2. However, at this temperature, the slope of $M(T)$ for both S1 and S2 changes, and below $^3T_{h\to e} = 70$ K, $M(T)$ starts to increase almost linearly, which continues up to the SC transition. It is interesting to note that in FeSe, at a temperature of $^3T_{h\to e} \sim 70$ K, $R_H(T)$ becomes negative again, and the charge carrier transition from holes to electrons finally occurs.[24,45] It is possible that under these circumstances, the magnetic and spin subsystems are somehow transformed, which leads to the observed linear growth of $M(T)$. The behavioral features of FeSe at a temperature of $^3T_{h\to e} \sim 70$ K are observed when measuring the magnetic susceptibility.[112] magnetoresistance,[112] Hall effect,[45,112] and relaxation time $1/(T_1T)$, as performed in nuclear magnetic resonance experiments.[113] Since all of these experiments involve a magnetic field, it is most likely that the observed features are caused by a transformation of the spin subsystem. Therefore, $^3T_{h\to e} \sim 70$ K can be considered as the onset temperature of enhanced anisotropic spin fluctuations, which induce the momentum-dependent anisotropy of charge carrier scattering rates over the Fermi surface.[63] This behavior can be considered as a certain transformation of the Fermi surface, which, as noted above, is a characteristic component of the pseudogap state.[4,14,49]

Let us note one more time that there are no features on the $\Delta^*(T)$ dependence of S2 at the onset temperature of enhanced anisotropic spin fluctuations $^3T_{h\to e} = 70$ (Fig. 5). This result is

consistent with the conclusions from Ref. 63 that the features at ${}^3T_{h\to e} \approx 70$ are observed in FeSe samples with high RRR values (=13.6 for S1), but are absent for samples with small RRR (=3.9 for S2) (Table I). Figure 5 shows that below T_s, the S2 $\Delta^*(T)$ parameter increases, demonstrating a broad maximum at $T_{max} \approx 53$ K, followed by a minimum at $T_{01} \approx 15$ K, a maximum at $T_0 \approx 8.9$ K, and a small minimum at $T_G \approx 8.4$ K (see the insert in Fig. 4). This is also clearly visible on Fig. 6, where the dependence $\Delta^*(T)$ is shown on a smaller scale. This shape of $\Delta^*(T)$ fully corresponds with the temperature dependence of the PG for cuprates.[52,82,90] Therefore, the obtained dependence $\Delta^*(T)$ indicates that it is possible for the PG state to implement in FeSe over the $T_s > T > T_c^{mf}$ interval, most likely due to the spin fluctuations which, as noted above, can contribute to the formation of paired fermions above T_c. This possibility is also noted in a number of articles.[24,45,46,51,63] As shown in our previous work,[67] $FeSe_{0.94}$ has a region of SC fluctuations near T_c, $\Delta T_{fl} = T_{01} - T_G$, where the FCPs behave like SC Cooper pairs, but without long-range order, with T_{01} being approximately two times higher than T_c. That is, $T_{01} \approx 20$–30 K, which is consistent with the results of Refs. 46 and 68. Note that in this case, there are no features along $R(T)$ all the way to T_s. In other words, if the FCPs are below T_{01}, then they must also exist at even higher temperatures of up to T_s. Based on these considerations, it is possible to make the assumption that below $T_s \sim 85$ K FCPs start to form in FeSe, which, as is the case in cuprates, suppress the DOS at the Fermi level[46,68,82,112] and contribute to the implementation of the PG (see Ref. 63, and references therein).

The dependence $\Delta^*(T)$ of sample S1 below T_s also has a maximum, the specific shape of which, as mentioned, is most likely caused by Ag additives. It is logical to assume that a PG also opens below T_s in S1, since with a further drop in temperature below T_{01}, S1 demonstrates the type of $\Delta^*(T)$ dependence that is associated with the PG and is observed in HTSCs in the SC fluctuation region (see the insert in Fig. 4). In turn, if the $\Delta^*(T)$ of S3, which should be pure together with S2, shows any signs of PG behavior below T_s, then they are very weakly expressed (Fig. 5). Most likely, inclusions of the nonsuperconducting hexagonal phase in S3 suppress the possibility of FCP formation below T_s. The same applies to the region of SC fluctuations below T_{01}, where, as already noted, the dependence $\Delta^*(T)$ for S3 is very different from the dependence that is typical for most HTSCs (see the insert in Fig. 4). It is also interesting to note that the $\Delta^*(T)$ of the Fe-pnictide $EuFeAsO_{0.85}F_{0.15}$ has no maximum, and therefore no PG, in this temperature range (see Fig. 6 in Ref. 23), since the case of the PG opens at $T^* = 171$ K. This result emphasizes the noticeable difference between the PG state implementation in FeSe and Fe-pnictides.

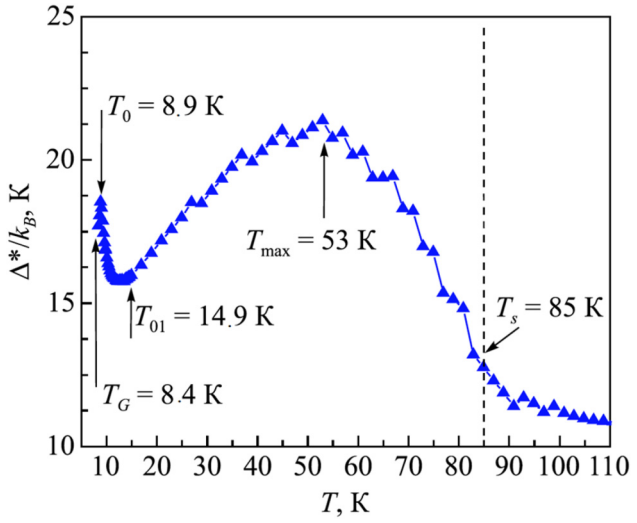

FIG. 6. The temperature dependence of parameter $\Delta^*(T)/k_B$ for S2, in the range from T_c^{mf} to T_s. The arrows indicate the corresponding characteristic temperatures (see text).

Therefore, it is most likely that the FCPs formed below T_s are what determine the SC transition mechanism of FeSe. In fact, at $T > T_s$, the magnetic field does not affect $\rho(T)$ in any way. Whereas below T_s, the magnetic field noticeably increases the resistivity of FeSe samples[45,46] and references therein). This result is easy to explain, if we assume that the magnetic field destroys the FCPs formed below T_s. In addition, below T_s is precisely where Kohler's rule is violated, indicating that there is a possible rearrangement of the Fermi surface,[45,63] which, as noted above, is the main sign of the PG state in HTSCs. Interestingly, the scaling behavior of the magnetoresistance, which follows from Kohler's rule, is restored below $T \approx 25$ K $\approx T_{01}$,[45,63] i.e., in the SC fluctuation region.[67] Thus, it seems reasonable to conclude that the FS stabilizes before the SC transition.

Figure 7 compares the dependences $\Delta^*(T)/\Delta^*_{max}$ of samples S1, S2, and S3 near T_c (see the insert in Fig. 4) with the temperature dependences of the local pair density in HTSC $<n\uparrow n\downarrow>$ calculated in the Peters–Bauer theory (PB)[73] within the framework of the three-dimensional attractive Hubbard model for different temperatures T/W, interactions U/W, and filling factor, where W is the band width. This makes it possible to estimate the value $<n\uparrow n\downarrow>$ in all three FeSe samples at T_G. To do this, we combine the measured values of Δ^*/Δ^*_{max} for S2 at T_G with the minimum, and at T_0 with the maximum, of each theoretical curve calculated at various U/W values, thus achieving the best agreement between the experiment and theory over the widest possible temperature range. It is important that the fitting coefficients found for S2 also be used for the other two samples. The fitting results for the three U/W values are shown in Fig. 7. Sample S2 (triangles) shows excellent agreement with the theory at $U/W = 0.2$ (curve 1) over almost the entire SC fluctuation range. The obtained value $<n\uparrow n\downarrow>(T_G) \approx 0.29$ is practically the same as in YBCO. It can be seen that the maximum value $<n\uparrow n\downarrow>(T_G) \approx 0.47$ is demonstrated by sample S1 doped with Ag. At the same time, the experimental values of $\Delta^*(T)$ (points) coincide with the theory at $U/W = 1{,}2$ (curve 4) over a wide temperature range above T_c. Note that $<n\uparrow n\downarrow>(T_G) \approx 0.47$ is noticeably larger than $<n\uparrow n\downarrow>(T_G) \approx 0.3$, which we obtained for optimally doped YBaCuO single crystals.[114] This somewhat unexpected result can be considered as a consequence of the Ag impurity, which improves both the internal and intergranular SC properties of FeSe.[74,78,79] In turn, the dependence $\Delta^*(T)$ of sample S3 (squares) does not coincide with the PB theory. Accordingly, the local pair density in S3, $<n\uparrow n\downarrow>(T_G) \approx 0.26$, turned out to be the

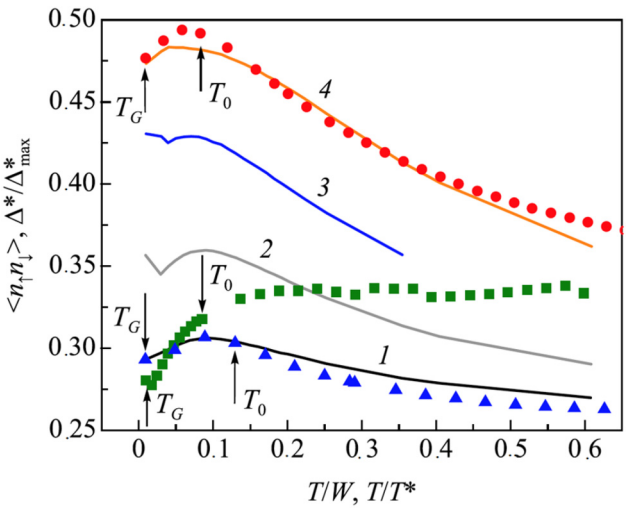

FIG. 7. Curves of Δ^*/Δ^*_{max} as functions T/T^* for $FeSe_{0.94}$ samples S1 (dots), S2 (triangles), and S3 (squares) in comparison with the theoretical curves of $<n\uparrow n\downarrow>$ as functions of T/W, at the corresponding interaction values U/W : 0.2 (1); 0.4 (2); 0.7 (3); 1.2 (4). The arrows indicate the temperatures T_0 and T_G.

smallest of the studied samples, as expected. Thus, the obtained results show that the various defective ensembles arising in $FeS0e_{0.94}$ polycrystalline samples with various manufacturing methods significantly affect sample properties.

CONCLUSION

For the first time, temperature dependence of the excess conductivity $\sigma'(T)$ is studied in three polycrystalline samples of the $FeSe_{0.94}$ superconductor, S1, S2, and S3, prepared using different technologies. From the data obtained in the local pair model, the calculated temperature dependences of the $\Delta^*(T)$ parameter, which is associated with the pseudogap in cuprates, turned out to be very informative. The ratio $2\Delta^*/k_BT_c = 4.6 \pm 0.2$ for S2 is in complete agreement with the results of heat capacity,[107] Andreev spectroscopy,[105] and muon-spin rotation[106] measurements. Moreover, a comparison with the results of our last work shows that the SC energy gap in $FeSe_{0.94}$ corresponds to the two-gap s + s model and, most likely, does not contain zeros.

It is shown that at high temperatures, the $\Delta^*(T)$ of the three samples has a shape that is characteristic of magnetic superconductors (Fe-pnictides), with a narrow maximum at $T_{s1} \sim 250$ K and a long linear region decreasing to $T \approx 225$ K (Fig. 5). Importantly, the distinct features on the magnetization $M(T)$ of samples S1 and S2 that are visible at T_{s1} indicate that the rearrangement of the $FeSe_{0.94}$ magnetic subsystem most likely ends at this temperature. Below ~ 225 K, the samples' dependences $\Delta^*(T)$ vary greatly. The $\Delta^*(T)$ of S1 (4 wt.%Ag) and S3 (with nonsuperconducting hexagonal phase inclusions), prepared by partial melting, have a number of features in the form of minima and maxima that correlate with the temperatures at which features are also observed on the $M(T)$. Additionally, the Hall coefficient $R_H(T)$ changes signs several times with decreasing T, indicating that FeSe changes charge carrier type.[24,44,45]

At the same time, these features are completely absent in the $\Delta^*(T)$ dependence of the impurity-free sample S2, prepared via solid state reaction. Up to the structural transition temperature $T_s = 85$ K, S2 shows a smooth $\Delta^*(T)$ curve that is usual for the Fe-pnictide $EuFeAsO_{0.85}F_{0.15}$ with a close $T_c = 11.6$ K.[23] At $T_s = 85$ K, the $\Delta^*(T)$ of all samples have a minimum, but there are no matching features along $M(T)$, which is consistent with the idea of a nematic structural transition in FeSe at T_s.[3,16,18,24,41–46]

Below T_s, the S2 sample exhibits a broad maximum along $\Delta^*(T)$, which is atypical for Fe-pnictides. An analysis of the obtained dependence suggests the possible discovery of a pseudogap in the $T < T_s$ interval for this FeSe sample, as suggested in a number of articles.[24,45,46,63,82] It has been proposed that fluctuation Cooper pairs (FCPs) begin to form below T_s in FeSe, the presence of which explains the increase in these samples' resistance in a magnetic field, across this temperature range.[45,46] In addition, Kohler's rule is violated below T_s.[45,63,81] indicating that there is a possible rearrangement of Fermi surface, which is the main sign of the PG state in HTSCs.[4,49,82] It should be noted that the scaling behavior of magnetoresistance, which follows from Kohler's rule, is restored below $T \approx 25$ K $\approx T_{01}$,[45,63] i.e., in the SC fluctuation region.[67] Based on this result, it can be assumed that FS stabilization occurs before the SC transition, which seems reasonable.

Below T_s, the S1 sample also exhibits a $\Delta^*(T)$ shape that resembles a pseudogap, but is altered by the impact of Ag impurities. At ${}^3T_{h\to e} \sim 70$ K, there is a nonsymmetric maximum, below which $\Delta^*(T)$ decreases linearly with temperature to T_{01} (Fig. 5). At the same time, S2 has no features along $\Delta^*(T)$ at $T \sim 70$ K. This result is consistent with the conclusions of Ref. 63, that the features at ${}^3T_{h\to e} \approx 70$ K are observed in FeSe samples with large RRR values (=13.6 for S1), but are absent in samples with small RRR (=3. 9 for S2) (Table I). Below $T \sim 70$ K, there is an almost linear increase in the $M(T)$ of both S1 and S2, which continues until the SC transition. It is interesting to note that at the FeSe temperature ${}^3T_{h\to e} \sim 70$ K, indicated by the dotted line in Fig. 5, $R_H(T)$ becomes negative once again, and the charge carrier type finally changes from holes to electrons.[24,45] It is possible that, at the same time, the observed linear growth of $M(T)$ is caused by a spin subsystem transformation (see Ref. 63, and the references therein). Below T_s, the dependence $\Delta^*(T)$ for the S3 sample has almost no maximum, which suggests that the nonsuperconducting impurities of the hexagonal phase prevent the formation of paired fermions in S3, near T_c. It is also interesting to note that no maximum along $\Delta^*(T)$, and therefore no pseudogap opening, are observed in this temperature range for the Fe-pnictide $EuFeAsO_{0.85}F_{0.15}$ (see Fig. 6 in Ref. 23), since in this case, the PG opens at $T^* = 171$ K. This result emphasizes the noticeable difference between implementing the PG state in FeSe and in Fe-pnictides.

The local pair density $<n\uparrow n\downarrow>$ of all samples (Fig. 7) is determined by comparing the $\Delta^*(T)$ near T_c with the Peters–Bauer theory.[73] For samples S1 and S2, the experimental values of $\Delta^*(T)$ coincide with the theory at $U/W = 1{,}2$ (S1) and 0,2 (S2) over a wide temperature range above T_c, which serves as evidence of the samples' high quality structure. The maximum $<n\uparrow n\downarrow>(T_G) \approx 0.47$ is obtained for the S1 sample. This is noticeably larger than $<n\uparrow n\downarrow>$

$(T_G) \approx 0.3$, which we obtained for optimally doped YBCO single crystals.[114] This somewhat unexpected result can be attributed to the impact of Ag impurities.[74,76,77] The value $<n \uparrow n \downarrow> (T_G) \approx 0.29$, found for S2 without impurities, is almost the same as in YBCO. This result allows us to discuss a common mechanism for the formation of FCPs near T_c, in various undoped HTSCs. The dependence $\Delta^*(T)$ of the S3 sample does not coincide with the PB theory, likely due to the distortions of the crystal lattice caused by the impurities of the nonsuperconducting hexagonal phase. As expected, the local pair density $<n \uparrow n \downarrow> (T_G) \approx 0.26$ turned out to be the smallest of all three studied samples. The overall results obtained in this study show that the different defect ensembles occurring in $FeSe_{0.94}$ polycrystalline samples as a result of various manufacturing methods have a significant impact on sample properties.

ACKNOWLEDGMENTS

The authors are grateful to S. I. Bondarenko and V. P. Gnezdilov for the helpful deliberations. This work was partially supported by the research project collaboration between the Ukrainian and Polish, as well as the Polish and Bulgarian, Academies of Sciences.

REFERENCES

[1]E. V. L. de Mello, M. T. D. Orlando, J. L. Gonzalez, E. S. Caixeiro, and E. Baggio-Saitovich, Phys. Rev. B **66**, 092504 (2002).
[2]L. J. Shen, C. C. Lam, J. Q. Li, J. Feng, Y. S. Chen, and H. M. Shao, Supercond. Sci. Technol. **11**, 1277 (1998).
[3]V. M. Loktev, R. M. Quick, and S. G. Sharapov, Phys. Rep. **349**, 1 (2001).
[4]Y. Y. Peng, R. Fumagalli, Y. Ding, M. Minola, S. Caprara, D. Betto, M. Bluschke, G. M. De Luca, K. Kummer, E. Lefrançois, M. Salluzzo, H. Suzuki, M. Le Tacon, X. J. Zhou, N. B. Brookes, B. Keimer, L. Braicovich, M. Grilli, and G. Ghiringhelli, Nat. Mater. **17**, 697 (2018).
[5]J. Gao, J. W. Park, K. Kim, S. K. Song, F. Chen, X. Luo, Y. Sun, and H. W. Yeom, arXiv:1904.04508 (2019).
[6]J. L. Tallon, J. G. Storey, J. R. Cooper, and J. W. Loram, arXiv:1907.12018v1 (2019).
[7]M. Grandadam, D. Chakraborty, and C. Pepin, arXiv:1909.06657v1 (2019).
[8]I. Esterlis, S. A. Kivelson, and D. J. Scalapino, Phys. Rev. B **99**, 174516 (2019).
[9]G. Yu, D.-D. Xia, D. Pelc, R.-H. He, N.-H. Kaneko, T. Sasagawa, Y. Li, X. Zhao, N. Barišić, A. Shekhter, and M. Greven, Phys. Rev. B **99**, 214502 (2019).
[10]X. Wang, Q. Chen, and K. Levin, arXiv:1907.06121v1 (2019).
[11]A. L. Solovjov, "Pseudogap and local pairs in high-Tc superconductors," in *Superconductors — Materials, Properties and Applications*, edited by A. Gabovich (InTech, Rijeka, 2012), Chapter 7, p. 137.
[12]T. Timusk and B. Statt, Rep. Prog. Phys. **62**, 161 (1999) arXiv:cond-mat/9905219.
[13]M. V. Sadovskii, Physics-Uspekhi **51**, 1201 (2008).
[14]S. Badoux, W. Tabis, F. Laliberte, G. Grissonnanche, B. Vignolle, D. Vignolles, J. Beard, D. A. Bonn, W. N. Hardy, R. Liang, N. Doiron-Leyraud, L. Taillefer, and C. Proust, Nature (London) **531**, 210 (2016).
[15]Y. Kamihara, T. Watanabe, M. Hirano, and H. Hosono, J. Am. Chem. Soc. **130**, 3296 (2008).
[16]Z. A. Ren, J. Yang, W. Lu, W. Yi, X. L. Shen, Z. C. Li, G. C. Che, X. L. Dong, L. L. Sun, F. Zhou, and Z. X. Zhao, Europhys. Lett. **82**, 57002 (2008).
[17]C. Wang, L. J. Li, S. Chi, Z. W. Zhu, Z. Ren, Y. K. Li, Y. T. Wang, X. Lin, Y. K. Luo, S. A. Jiang, X. F. Xu, G. H. Cao, and Z. A. Xu, Europhys. Lett. **83**, 67006 (2008).
[18]Y. V. Pustovit and A. A. Kordyuk, Fiz. Nizk. Temp. **42**, 1268 (2016) [Low Temp. Phys. **42**, 995 (2016)].
[19]S. Karlsson, P. Strobel, A. Sulpice, C. Marcenat, M. Legendre, F. Gay, S. Pairis, O. Leynaud, and P. Toulemonde, Supercond. Sci. Technol. **28**, 105009 (2015).
[20]C.-J. Liu, A. Bhaskar, H.-J. Huang, and F.-H. Lin, Appl. Phys. Lett. **104**, 252602 (2014).
[21]A. L. Solovjov, L. V. Omelchenko, R. V. Vovk, O. V. Dobrovolskiy, Z. F. Nazyrov, S. N. Kamchatnaya, and D. M. Sergeyev, Physica B **493**, 58 (2016).
[22]Y. Ando, S. Komiya, K. Segawa, S. Ono, and Y. Kurita, Phys. Rev. Lett. **93**, 267001 (2004).
[23]A. L. Solovjov, L. V. Omelchenko, A. V. Terekhov, K. Rogacki, R. V. Vovk, E. P. Khlybov, and A. Chroneos, Mater. Res. Express **3**, 076001 (2016).
[24]Y. Sun, S. Pyon, T. Tamegai, R. Kobayashi, T. Watashige, S. Kasahara, Y. Matsuda, and T. Shibauchi, Phys. Rev. B **92**, 144509 (2015).
[25]E. Pomjakushina, K. Conder, V. Pomjakushin, M. Bendele, and R. Khasanov, Phys. Rev. B **80**, 024517 (2009).
[26]Y. Mizuguchi, F. Tomioka, S. Tsuda, T. Yamaguchi, and Y. Takano, Appl. Phys. Lett. **93**, 152505 (2008).
[27]S. Medvedev, T. M. McQueen, I. A. Troyan, T. Palasyuk, M. I. Eremets, R. J. Cava, S. Naghavi, F. Casper, V. Ksenofontov, G. Wortmann, and C. Felse, Nat. Mater. **8**, 630 (2009).
[28]Y. Mizuguchi and Y. Takano, J. Phys. Soc. Jpn. **79**, 102001 (2010).
[29]M. H. Fang, H. M. Pham, B. Qian, T. J. Liu, E. K. Vehstedt, Y. Liu, L. Spinu, and Z. Q. Mao, Phys. Rev. B **78**, 224503 (2008).
[30]L. Sun, X.-J. Chen, J. Guo, P. Gao, Q.-Z. Huang, H. Wang, M. Fang, X. Chen, G. Chen, Q. Wu, C. Zhang, D. Gu, X. Dong, L. Wang, K. Yang, A. Li, X. Dai, H.- . Mao, and Z. Zhao, Nature **483**, 67 (2012).
[31]J.-F. Ge, Z.-L. Liu, C. Liu, C.-L. Gao, D. Qian, Q.-K. Xue, Y. Liu, and J.-F. Jia, Nat. Mater. **14**, 285 (2015).
[32]Q.-Y. Wang, Z. Li, W.-H. Zhang, Z.-C. Zhang, J.-S. Zhang, W. Li, H. Ding, Y.-B. Ou, P. Deng, and K. Chang, Chin. Phys. Lett. **29**, 037402 (2012).
[33]D. Liu, W. Zhang, D. Mou, J. He, Y.-B. Ou, Q.-Y. Wang, Z. Li, L. Wang, L. Zhao, S. He, Y. Peng, X. Liu, C. Chen, L. Yu, G. Liu, X. Dong, J. Zhang, C. Chen, Z. Xu, J. Hu, X. Chen, X. Ma, Q. Xue, and X. J. Zhou, Nat. Commun. **3**, 931 (2012).
[34]I. Bozovic and C. Ahn, Nat. Phys. **10**, 892 (2014).
[35]P. L. Bach, S. R. Saha, K. Kirshenbaum, J. Paglione, and R. L. Greene, Phys. Rev. B **83**, 212506 (2011).
[36]C. W. Luo, I. H. Wu, P. C. Cheng, J.-Y. Lin, K. H. Wu, T. M. Uen, J. Y. Juang, T. Kobayashi, D. A. Chareev, O. S. Volkova, and A. N. Vasiliev, Phys. Rev. Lett. **108**, 257006 (2012).
[37]V. Gnezdilov, Y. G. Pashkevich, P. Lemmens, D. Wulferding, T. Shevtsova, A. Gusev, D. Chareev, and A. Vasiliev, Phys. Rev. B **87**, 144508 (2013).
[38]S. Margadonna, Y. Takabayashi, M. T. McDonald, K. Kasperkiewicz, Y. Mizuguchi, Y. Takano, A. N. Fitch, E. Suard, and K. Prassides, Chem. Commun. (Cambridge) **43**, 5607 (2008).
[39]A. I. Coldea and M. D. Watson, Annu. Rev. Condens. Matter Phys. **9**, 125 (2018).
[40]I. A. Nekrasov, N. S. Pavlova, M. V. Sadovskii, and A. A. Slobodchikova, Fiz. Nizk. Temp. **42**, 1137 (2016) [Low Temp. Phys. **42**, 891 (2016)].
[41]J. P. Sun, G. Z. Ye, P. Shahi, J.-Q. Yan, K. Matsuura, H. Kontani, G. M. Zhang, Q. Zhou, B. C. Sales, T. Shibauchi, Y. Uwatoko, D. J. Singh, and J.-G. Cheng, Phys. Rev. Lett. **118**, 147004 (2017).
[42]P. Massat, D. Farina, I. Paul, S. Karlsson, P. Strobel, P. Toulemonde, M.-A. Measson, M. Cazayous, A. Sacuto, S. Kasahara, T. Shibauchi, Y. Matsuda, and Y. Gallais, PNAS **113**, 9177 (2016).
[43]M. D. Watson, T. K. Kim, A. A. Haghighirad, N. R. Davies, A. McCollam, A. Narayanan, S. F. Blake, Y. L. Chen, S. Ghannadzadeh, A. J. Schoeld, M. Hoesch, C. Meingast, T. Wolf, and A. I. Coldea, Phys. Rev. B **91**, 155106 (2015).
[44]Y. J. Song, J. B. Hong, B. H. Min, K. J. Lee, M. H. Jung, J.-S. Rhyee, and Y. S. Kwon, J. Korean Phys. Soc. **59**, 312 (2011).
[45]Y. Sun, S. Pyon, and T. Tamegai, Phys. Rev. B **93**, 104502 (2016).
[46]S. Kasahara, T. Yamashita, A. Shi, R. Kobayashi, Y. Shimoyama, T. Watashige, K. Ishida, T. Terashima, T. Wolf, F. Hardy, C. Meingast, H. Löhneysen, A. Levchenko, T. Shibauchi, and Y. Matsuda, Nat. Commun. **7**, 12843 (2016).

[47]M. Randeria, Nat. Phys. **6**, 561 (2010).
[48]W. Lang, G. Heine, P. Schwab, X. Z. Wang, and D. Bauerle, Phys. Rev. B **49**, 4209 (1994).
[49]L. Taillefer, Annu. Rev. Condens. Matter Phys. **1**, 51 (2010).
[50]S. Dzhumanov, E. X. Karimboev, U. T. Kurbanov, and O. K. Ganiev, S. S. Djumanov, Superlattices and Microstruct. **68**, 6 (2014).
[51]B. P. Stojkovic and D. Pines, Phys. Rev. B **55**, 8576 (1997).
[52]A. L. Solovjov, L. V. Omelchenko, V. B. Stepanov, R. V. Vovk, H.-U. Habermeier, H. Lochmajer, P. Przyslupski, and K. Rogacki, Phys. Rev. B **94**, 224505 (2016).
[53]L. G. Aslamazov and A. L. Larkin, Phys. Lett. A **26**, 238 (1968).
[54]S. Hikami and A. I. Larkin, Mod. Phys. Lett. B **2**, 693 (1988).
[55]J. Corson, R. Mallozzi, J. Orenstein, J. N. Eckstein, and I. Bozovic, Nature (London) **398**, 221 (1999).
[56]K. Kawabata, S. Tsukui, Y. Shono, O. Michikami, H. Sasakura, K. Yoshiara, Y. Kakehi, and T. Yotsuya, Phys. Rev. B **58**, 2458 (1998).
[57]Y. Yamada, K. Anagawa, T. Shibauchi, T. Fujii, T. Watanabe, A. Matsuda, and M. Suzuki, Phys. Rev. B **68**, 054533 (2003).
[58]V. J. Emery and S. A. Kivelson, Nature (London) **374**, 434 (1995).
[59]P. G. DeGennes, *Superconductivity of Metals and Alloys* (W. A. Benjamin Inc., New York, Amsterdam, 1996), P. 280.
[60]M. S. Grbic, M. Pozek, D. Paar, V. Hinkov, M. Raichle, D. Haug, B. Keimer, N. Baricic, and A. Dulcic, Phys. Rev. B **83**, 144508 (2011).
[61]I. Pallecchi, M. Tropeano, C. Ferdeghini, G. Lamura, A. Martinelli, A. Palenzona, and M. Putti, J. Supercond. Nov. Magn. **24**, 1751 (2011).
[62]P. Mishra, H. Lohani, R. A. Zargar, V. P. S. Awana, and B. R. Sekhar, AIP Conf. Proc. 1665, 130015 (2015).
[63]S. Rößler, C.-L. Huang, L. Jiao, C. Koz, U. Schwarz, and S. Wirth, Phys. Rev. B **97**, 094503 (2018).
[64]L. Craco, M. S. Laad, and S. Leoni, J. Phys. Conf. Ser. **487**, 012017 (2014).
[65]A. Yamasaki, Y. Matsui, S. Imada, K. Takase, H. Azuma, T. Muro, Y. Kato, A. Higashiya, A. Sekiyama, S. Suga, M. Yabashi, K. Tamasaku, T. Ishikawa, K. Terashima, H. Kobori, A. Sugimura, N. Umeyama, H. Sato, Y. Hara, N. Miyagawa, and S. I. Ikeda, Phys. Rev. B **82**, 184511 (2010).
[66]R. Yoshida, T. Wakita, H. Okazaki, Y. Mizuguchi, S. Tsuda, Y. Takano, H. Takeya, K. Hirata, T. Muro, M. Okawa, K. Ishizaka, S. Shin, H. Harima, M. Hirai, Y. Muraoka, and T. Yokoya, J. Phys. Soc. Jpn. **78**, 034708 (2009).
[67]A. L. Solovjov, E. V. Petrenko, V. B. Stepanov, E. Nazarova, K. Buchkov, and K. Rogacki, submitted to *Phys. Rev. B*.
[68]Y. G. Naidyuk, N. V. Gamayunova, O. E. Kvitnitskaya, G. Fuchs, D. A. Chareev, and A. N. Vasiliev, Fiz. Nizk. Temp. **42**, 42 (2016) [Low Temp. Phys. **42**, 31 (2016)].
[69]H. Alloul, T. Ohno, and P. Mendels, Phys. Rev. Lett. **63**, 1700 (1989).
[70]T. Kondo, A. D. Palczewski, Y. Hamaya, T. Takeuchi, J. S. Wen, Z. J. Xu, G. Gu, and A. Kaminski, Phys. Rev. Lett. **111**, 157003 (2013).
[71]A. Shi, T. Arai, S. Kitagawa, T. Yamanaka, K. Ishida, A. E. Bohmer, C. Meingast, T. Wolf, M. Hirata, and T. Sasaki, J. Phys. Soc. Jpn. **87**, 013704 (2018).
[72]A. L. Solovjov, A. V. Terekhov, E. V. Petrenko, L. V. Omelchenko, and Z. Cuiping, FNT **45**, 1403 (2019) [Low Temp. Phys. **45**, 1193 (2019)].
[73]R. Peters and J. Bauer, Phys. Rev. B **92**, 014511 (2015).
[74]E. Nazarova, N. Balchev, K. Nenkov, K. Buchkov, D. Kovacheva, A. Zahariev, and G. Fuchs, Supercond. Sci. Technol. **28**, 025013 (2015).
[75]P. Rani, A. Pal, and V. P. S. Awana, Physica C **497**, 19 (2014).
[76]R. Mawassi, S. Marhaba, M. Roumié, R. Awad, M. Korek, and I. Hassan, J. Supercond. Nov. Magn. **27**, 1131 (2014).
[77]K. Fabitha, M. S. Ramachandra Rao, M. Muralidhar, K. Furutani, and M. Murakami, J. Supercond. Nov. Magn. **30**, 3117 (2017).
[78]A. Galluzzi, M. Polichetti, K. Buchkov, E. Nazarova, D. Mancusi, and S. Pace, Supercond. Sci. Technol. **30**, 025013 (2017).
[79]E. Nazarova, K. Buchkov, S. Terzieva, K. Nenkov, A. Zahariev, D. Kovacheva, N. Balchev, and G. Fuchs, J. Supercond. Nov. Magn. **28**, 1135 (2015).
[80]N. Chen, Z. Ma, Y. Liu, X. Li, and Q. Cai, "H. Li and L. Yu," J. Alloys Compd. **588**, 418 (2014).
[81]E. Nazarova, N. Balchev, K. Buchkov, K. Nenkov, D. Kovacheva, D. Gajda, and G. Fuchs, in *High-Temperature Superconductors: Occurrence, Synthesis and Applications*, edited by M. Miryala and M. R . Koblischka (Nova Science Publishers, 2018), Chap. 8, p. 195.
[82]A. L. Solovjov and V. M. Dmitriev, FNT **32**, 139 (2006) [Low Temp. Phys. **32**, 99 (2006)].
[83]A. L. Solovjov, H.-U. Habermeier, and T. Haage, FNT **28**, 24 (2002) [Low Temp. Phys. 28, 17 (2002)].
[84]B. Oh, K. Char, A. D. Kent, M. Naito, M. R. Beasley, T. H. Geballe, R. H. Hammond, A. Kapitulnik, and J. M. Graybeal, Phys. Rev. B **37**, 7861 (1988).
[85]V. L. Ginzburg and L. D. Landau, "On the theory of superconductivity," in *On Superconductivity and Superfluidity* (Springer, Berlin, Heidelberg, 2009).
[86]E. M. Lifshitz and L. P. Pitaevski, *Statistical Physics* (Nauka, Moscow, 1978).
[87]A. Kapitulnik, M. R. Beasley, C. Castellani, and C. Di Castro, Phys. Rev. B **37**, 537 (1988).
[88]T. Schneider and J. M. Singer, *Phase Transition Approach to High-Temperature Superconductivity: Universal Properties of Cuprate Superconductors* (Imperial College Press, London, 2000).
[89]B. Leridon, A. Defossez, J. Dumont, J. Lesueur, and J. P. Contour, Phys. Rev. Lett. **87**, 197007 (2001).
[90]A. L. Solovjov and V. M. Dmitriev, FNT **35**, 227 (2009) [Low Temp. Phys. **35**, 169 (2009)].
[91]J. Stajic, A. Iyengar, K. Levin, B. R. Boyce, and T. R. Lemberger, Phys. Rev. B **68**, 024520 (2003).
[92]D. S. Inosov, J. T. Park, A. Charnukha, Y. Li, A. V. Boris, B. Keimer, and V. Hinkov, Phys. Rev. B **83**, 214520 (2011).
[93]Ø Fischer, M. Kugler, I. Maggio-Aprile, and C. Berthod, Rev. Mod. Phys. **79**, 353 (2007).
[94]A. I. D'yachenko, V. Y. Tarenkov, V. V. Kononenko, E. M. Rudenko, Metallofiz. Noveishie Tekhnol. **38**(5), 565–599 (2016).
[95]J. P. Carbotte, T. Timusk, and J. Hwang, Rep. Prog. Phys. **74**, 066501 (2011).
[96]E. G. Maksimov, M. L. Kulić, and O. V. Dolgov, Adv. Condens. Matter. Phys. (2010), Article ID 423725 (2010).
[97]G.-. Zhao, Physica Scripta **83**, 038302 (2011).
[98]M. R. Norman, in *Novel Superfluids*, edited by K. H. Bennemann and J. B. Ketterson (Oxford University Press, 2013).
[99]D. J. Scalapino, Rev. Mod. Phys. **84**, 1383 (2012).
[100]C. Berthod, Y. Fasano, I. Maggio-Aprile, A. Piriou, E. Giannini, G. Levy de Castro, And Ø. Fischer, Phys. Rev. B **88**, 014528 (2013).
[101]S. Ideta, T. Yoshida, A. Fujimori, H. Anzai, T. Fujita, A. Ino, M. Arita, H. Namatame, M. Taniguchi, Z.-X. Shen, K. Takashima, K. Kojima, and S. Uchida, Phys. Rev. B **85**, 104515 (2012).
[102]J. W. Alldredge, K. Fujita, H. Eisaki, S. Uchida, and K. McElroy, Phys. Rev. B **87**, 104520 (2013).
[103]T. Kurosawa, T. Yoneyama, Y. Takano, M. Hagiwara, R. Inoue, N. Hagiwara, K. Kurusu, K. Takeyama, N. Momono, M. Oda, and M. Ido, Phys. Rev. B **81**, 094519 (2010).
[104]A. Pushp, C. V. Parker, A. N. Pasupathy, K. K. Gomes, S. Ono, J. Wen, Z. Xu, G. Gu, and A. Yazdani, Science **324**, 1689 (2009).
[105]Y. G. Ponomarev, S. A. Kuzmichev, M. G. Mikheev, M. V. Sudakova, S. N. Tchesnokov, T. E. Shanygina, O. S. Volkova, A. N. Vasiliev, and T. Wolf, JETP **113**, 459 (2011).
[106]R. Khasanov, K. Conder, E. Pomjakushina, A. Amato, C. Baines, Z. Bukowski, J. Karpinski, S. Katrych, H.-H. Klauss, H. Luetkens, A. Shengelaya, and N. D. Zhigadlo, Phys. Rev. B **78**, 220510(R) (2008).
[107]Y. Sun, S. Kittaka, S. Nakamura, T. Sakakibara, K. Irie, T. Nomoto, K. Machida, J. Chen, and T. Tamegai, Phys. Rev. B **96**, 220505(R) (2017).

[108]A. Subedi, L. Zhang, D. J. Singh, and M. H. Du, Phys. Rev. B **78**, 134514 (2008).
[109]A. L. Solovjov, V. N. Svetlov, V. B. Stepanov, and S. L. Sidorov, V. Y. Tarenkov, A. I. Dyachenko, and A. B. Agafonov, Fiz. Nizk. Temp. **37**, 703 (2011) [Low Temp. Phys. **37**, 557 (2011)].
[110]T. M. McQueen, A. J. Williams, P. W. Stephens, J. Tao, Y. Zhu, V. Ksenofontov, F. Casper, C. Felser, and R. J. Cava, Phys. Rev. Lett. **103**, 057002 (2009).
[111]R. M. Fernandes, A. V. Chubukov, and J. Schmalian, Nat. Phys. **10**, 97 (2014).
[112]S. Rößler, C. Koz, L. Jiao, U. K. Rößler, F. Steglich, U. Schwarz, and S. Wirth, Phys. Rev. B **92**, 060505(R) (2015).
[113]T. Imai, K. Ahilan, F. L. Ning, T. M. McQueen, and R. J. Cava, Phys. Rev. Lett. **102**, 177005 (2009).
[114]A. L. Solovjov, E. V. Petrenko, L. V. Omelchenko, R. V. Vovk, I. L. Goulatis, and A. Chroneos, Sci. Rep. **9**, 9274 (2019).

Translated by AIP Author Services